(NASA-CR-169706) MECHANISM OF HOT CORROSION N83-15411
IN-738 Final Report (Pittsburgh Univ.)
p HC A02/MF A01 CSCL 11F
Unclas
G3/26 02331

METALLURGICAL AND MATERIALS ENGINEERING

University of Pittsburgh
Pittsburgh, Pennsylvania 15261

MECHANISM OF HOT
CORROSION OF IN-738

Final Report
on
Grant No. NSG-3214

Prepared for

National Aeronautics and Space Administration

by

G. H. Meier
Department of Metallurgical and Materials Engineering
University of Pittsburgh
Pittsburgh, Pennsylvania 15261

December 9, 1982

ABSTRACT

Previous work has shown that the Na_2SO_4 - induced hot corrosion of In-738 in the temperature range 900-1000°C is characterized by an initiation stage during which the corrosion rate is slow followed by a propagation stage during which the corrosion rate is markedly accelerated. Further work, to be presented in this report, has indicated that the corrosion process is, in fact, characterized by three fairly distinct stages. In Stage I the rate is similar to that in simple oxidation while in Stage II it is accelerated due essentially to a sulfidation/oxidation mechanism, and in Stage III, the rate becomes catastrophic due to acid fluxing induced by an accumulation of refractory metal oxides (particularly MoO_3) in the Na_2SO_4. The sequential stages in the corrosion process will be described and a mechanism proposed. The influence of alloy microstructure on the corrosion mechanism will also be discussed.

INTRODUCTION

The nickel-base superalloy IN-738 is widely used in gas turbine engines because it has good mechanical properties and hot corrosion resistance which is superior to that of most nickel-base alloys. Therefore, an understanding of the oxidation and hot corrosion behavior of this type of alloy is desirable.

The oxidation of IN-738 in air or oxygen has been studied by a number of investigators[1-7]. The isothermal oxidation is found to be essentially parabolic at temperatures around 1000°C. The external scale is essentially Cr_2O_3 which is covered with a thin layer of TiO_2. Small amounts of a complex oxide of the type $NiTaO_6$ have also been detected. Needle-like internal oxides, which are essentially Al_2O_3, are observed in the alloy and grow normal to the alloy/oxide interface. The scales formed on IN-738 are observed to spall extensively during thermal cycling which leads to large weight losses.

The Na_2SO_4 - induced hot corrosion of IN-738 has also been studied by a number of investigators[1,8-16]. This work has shown the hot corrosion degradation in the temperature range 900-1000°C is characterized by two stages: an initiation stage during which the corrosion rate is little different from that in simple oxidation and a propagation stage during which the corrosion is markedly accelerated. The length of the incubation period was observed to be a minimum at a temperature of about 975°C[16].

The hot corrosion attack of IN-738 has been observed to be quite sensitive to the metallurgical structure of the alloy[14-17]. Preoxidation of IN-738 has been observed to greatly lengthen the initiation time with respect to its temperature dependence[13]. It has also been observed that greater thicknesses of the preformed scale result in longer initiation times[13].

This report presents the results of a study of the initiation and propagation of the hot corrosion of cast IN-738 and the effect of metallurgical structure on these reactions.

EXPERIMENTAL

The alloy studied was IN-738 (Ni-16 w/o Cr-3.4 w/o Al-3.4 w/o Ti-8.5 w/o Co-1.75 w/o Mo-2.6 w/o W-1.75 w/o Ta-0.9 w/o Nb-0.17 w/o C-0.10 w/o Zr-0.01 w/o B) which was provided by the International Nickel Company (INCO) in the form of a 7 cm diameter, vacuum-cast cylinder. The macrostructure of the ingot is shown in Figure 1. Specimens were cut from three locations in the ingot (a) the columnar zone extending up from the chill zone at the bottom of the ingot, (b) the central region which contained large equiaxed grains and (c) the columnar zone extending radially inward from the cylindrical surface. The specimens were polished through 600 grit silicon carbide and ultrasonically cleaned. Coatings of Na_2SO_4 were applied by spraying an aqueous solution of Na_2SO_4 onto specimens which were heated using a hot plate and a heat lamp. Coating weights were generally 1 mg/cm^2.

A continuous reading Cahn RG microbalance was used to record weight changes at temperatures between 900 and 1000°C (the results presented here will be restricted to 970°C) in 1 atmosphere of slowly flowing oxygen. The reaction was initiated by raising a preheated furnace around the quartz tube in which the specimen was supported with oxygen flowing. The furnace was raised in a time period of ten seconds and thermal equilibrium was achieved in one to two minutes. Exposures of selected specimens were interrupted, the salt washed from the surface, and the exposure continued. Exposed specimens were studied using optical and scanning electron metallography (SEM) and x-ray diffraction.

RESULTS AND DISCUSSION

Previous work[14] has shown the Na_2SO_4-induced hot corrosion of IN-738 in the temperature range 900-100°C is characterized by two stages: an initiation stage during which the corrosion rate is little different from that in simple oxidation and a propagation stage during which the corrosion rate is markedly accelerated. The length of the initiation stage was found to vary with temperature having a minimum at about 970°C. A mechanism was proposed for the hot corrosion behavior[15,16] (Figure 2) and may be summarized as follows. Initially a thin, protective layer of Cr_2O_3 forms under the Na_2SO_4, Figure 2a. However, at the sites where alloy carbides, (Ti, Ta, Mo, W, Cb)C, intersect the surface there exist locally high concentrations of elements which, when oxidized and coming in contact with the molten salt, produce vary acid conditions. This results in the local dissolution of the scale and the penetration of the salt to the scale/alloy interface, Figure 2b. Here, since the salt is partially isolated from the atmosphere, the p_{O_2} will decrease and the p_{S_2} will increase. This results in the Al_2O_3 internal oxides becoming an essentially continuous Al_2O_3 layer and an increase in the density of sulfides which contain primarily Cr and Ti, Figure 2c. As this process continues the p_{S_2} continues to increase and refractory metal oxides are concentrated in the salt. The increased p_{S_2} results in the formation of massive Cr-sulfides, which are less stable than the Cr-Ti sulfides, in alloy grain boundaries, Figure 2d, and the eventual incorporation of entire grains of metal, which are now essentially pure Ni, into the scale where they are oxidized to produce the layered NiO scale characteristic of breakaway corrosion, Figure 2e.

Further work has indicated that the corrosion rate is, in fact, characterized by three fairly distinct stages and is very microstructure-dependent. The results of this work will now be described and related to the proposed mechanism for the hot corrosion of IN-738.

Figure 3 shows typical weight change vs. time behavior for IN-738 during hot corrosion at 970°C and indicates the three stages of the reaction. In Stage I the rate is similar to that for simple oxidation. In Stage II the rate is accelerated and in Stage III increases catastrophically. Figures 4 to 6 present typical corrosion morphologies at times indicated with arrows in Figure 3. During Stage I (Fig. 4-a and 4-b) the morphology is similar to that for oxidation consisting of an external scale of Cr_2O_3 and TiO_2 and internal precipitation of Al_2O_3. The major difference is the presence of small grey Cr, Ti-sulfides. Also during the early portion of this stage small amounts of Cr_2O_3 dissolve into the salt as sodium chromate.

During the accelerated Stage II (Figure 5) the external scale is thicker and chromium sulfides are observed at rather large depths in the alloy, particularly along alloy grain boundaries. Also during this stage considerable oxidation of the sulfides is observed. Therefore, it appears that the acceleration observed during Stage II is the result of a sulfidation/oxidation mechanism. The sulfidation results in localization of Cr in discrete sulfide particles which, upon oxidation, result in discrete Cr_2O_3 particles and limits the outward diffusion of Cr to maintain the external Cr_2O_3 layer. This causes the scale to become enriched in faster growing oxides.

The accelerated oxidation during Stage II results in the concentration of refractory metal oxides, particularly MoO_3, at the interface between the alloy and the corrosion product. This in turn gives rise to acidic fluxing and the catastrophic Stage III (Figure 6). This rapid corrosion produces a thick, porous scale comprised largely of NiO. The hot corrosion of IN-738 under these conditions then combines two propagation mechanisms in sequence: sulfidation/oxidation followed by acidic fluxing.

Figure 7 shows the result of an experiment to test part of the above mechanism. Two identical specimens were exposed until the rate had reached Stage II. At this point (4 hours) the salt was washed from one of the specimens. It was observed that the rate for this specimen continues to accelerate for a time via the sulfidation/oxidation mechanisms but then slows sharply. This result indicates that the sulfidation/oxidation reaction is not self-sustaining (for a fixed quantity of sulfur) and that the removal of the salt prevents the rapid acidic fluxing process from occurring. The role played by the sulfidation/oxidation reaction, therefore, is mainly in establishing the proper conditions for acidic fluxing to occur.

It was also observed that the hot corrosion process depended on the alloy structure. Figure 1 shows two sections through a cylindrical IN-738 ingot. Specimens were cut from location a. with the columnar grains normal to the plane of the specimen, from location b. in the equiaxed portion of the ingot, and from location c. with the columnar grains lying in the plane of the specimen. Figure 8 shows the microstructure of the three specimens and Figure 9 their rates of hot corrosion. It is clear that the specimen cut from the equiaxed region undergoes severe hot corrosion more rapidly than the specimens cut from the columnar region. This is believed to be due to the much larger carbides in the equiaxed region since, as discussed previously[15,16], the carbides play an important role in the initial penetration of the Cr_2O_3 scale and result in shorter incubation stages.

The two specimens cut from the columnar regions also exhibit different corrosion rates. This is believed due to specimen b. having a slightly larger carbide size and specimen a. having a large number of grain boundaries normal to the specimen surface to supply Cr to the Cr-depleted zone beneath the scale.

SUMMARY

The results presented in this report have shown that the hot corrosion degradation of IN-738 at 970°C consists of three stages. In Stage I the rate is similar to that in simple oxidation while in Stage II it is accelerated due essentially to a sulfidation/oxidation mechanism, and in Stage III, the rate becomes catastrophic due to acid fluxing induced by an accumulation of refractory metal oxides (particularly MoO_3) in the Na_2SO_4. The nature of the attack has also been shown to depend on the alloy microstructure.

REFERENCES

1. Y. Bourhis and C. St. John, Oxid. Met. 9, 507 (1975).

2. R. G. Garlick and C. E. Lowell, "Alloy Composition Effects on Oxidation Products of Vi A, B-1900, 713C and 738X - A High Temperature Diffractometer Study" NASA Technical Memorandum NASA TM X-2796, June 1973.

3. G. C. Fryburg, F. J. Kohl, and C. A. Stearns, "Oxidation in Oxygen at 900°C and 1000°C of Four Nickel-Base Cast Superalloys. NASA-TRW VI A, B-1900, Alloy 713C, and In-738", NASA Technical Note NASA Tn D-8388, January 1977.

4. S. R. Smith, W. J. Carter, III, G. D. Mateescu, F. J. Kohl, G. C. Fryburg, and C. A. Stearns, Oxid, Met. 14, 415 (1980).

5. C. A. Barrett, G. J. Santoro, and C. E. Lowell, "Isothermal and Cyclic Oxidation at 1000°C and 1100°C of Four Nickel-Base Alloys: NASA-TRW Vi A, B-1900, 713C, and 738X", NASA Technical Note NASA TN D-7484, Nov. 1973.

6. W. A. Sanders, "Dynamic Oxidation Behavior at 1000° and 1100°C of Four Nickel-Base Cast Alloys" NASA-TRW VI A, B-1900, 713 C, and 738X", NASA Technical Note NASA TN D-7682, Aug. 1974.

7. C. E. Lowell and H. B. Probst "Effects of Composition and Testing Conditions On Oxidation Behavior of Four Cast Commercial Nickel Base Superalloys", NASA Technical Note NASA TN D-7705, Sept. 1974.

8. G. C. Fryburg, F. J. Kohl, and C. A. Stearns "Hot Corrosion Studies of Four Nickel-Base Superalloys: B-1900, NASA-TRW VI A, 713C, and IN-738" in Properties of High Temperature Alloys, Z. A. Foroulis and F. S. Pettit eds. Electrochem. Soc., Princeton, NJ, 1976, p. 585.

9. E. Erdos and E. Denzler, "On the Oxidation and Hot Corrosion of IN-713-LC, IN-738 LC, and IN-939" in Behavior of High Temperature Alloys in Aggressive Environments", Proc. Int. Conf. Petten, The Netherlands, The Metals Soc., London, 1979, p. 455.

10. P. Cavallotti, V. Ducati, D. Colombo, and G. Donzelli, "Some Mechanisms of Scale Degradation in Hot Corrosion Experiments", Petten Conf. p. 513.

11. C. J. Grant, Br. Corros. J., 14, 26 (1979).

12. J. M. Ferguson and N. Jacob "The Effect of Pre-Sulphidation on the Oxidation Behavior of Gas Turbine Superalloys" RD/L/N74/80, Central Electricity Research Laboratories, Leatherhead, Surrey, U.K., Aug. 1980.

13. R. Haque, F. J. Kohl, G. E. Fryburg, C. A. Stearns, and W. L. Fielder, "Effects of Temperature and Oxide Scale Thickness on the Hot Corrosion of IN-738" to appear in Proc. of the Symp. on High Temperature Materials Chemistry, Electrochem Soc., Denver, Colorado, Oct. 11-16, 1981.

14. T. Huang, E. A. Gulbransen, and G. H. Meier, J. Metals, 31, 28 (1979).

15. T. T. Huang and G. H. Meier, "An Investigation of the Initiation Stage of Hot Corrosion in Ni-Base Alloys", University of Pittsburgh, Progress Repts. 1 and 2 on NASA Grant NSG-3214, March and November 1979.

16. T. T. Huang "An Investigation of Hot Corrosion Mechanisms of Some Nickel-Base Alloys", Ph.D. Thesis, University of Pittsburgh (1979).

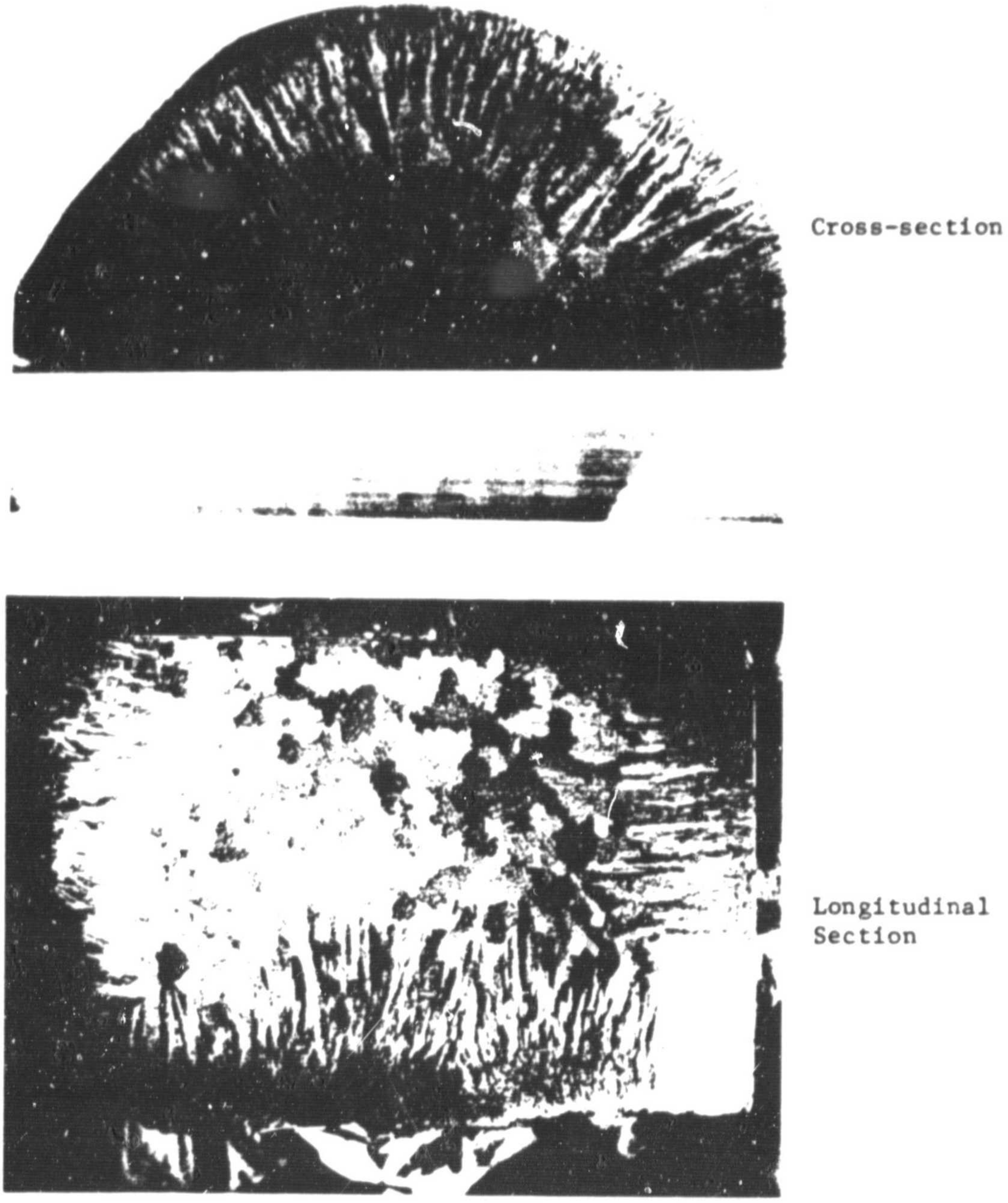

Figure 1 Macrostructure of IN-738 Ingot

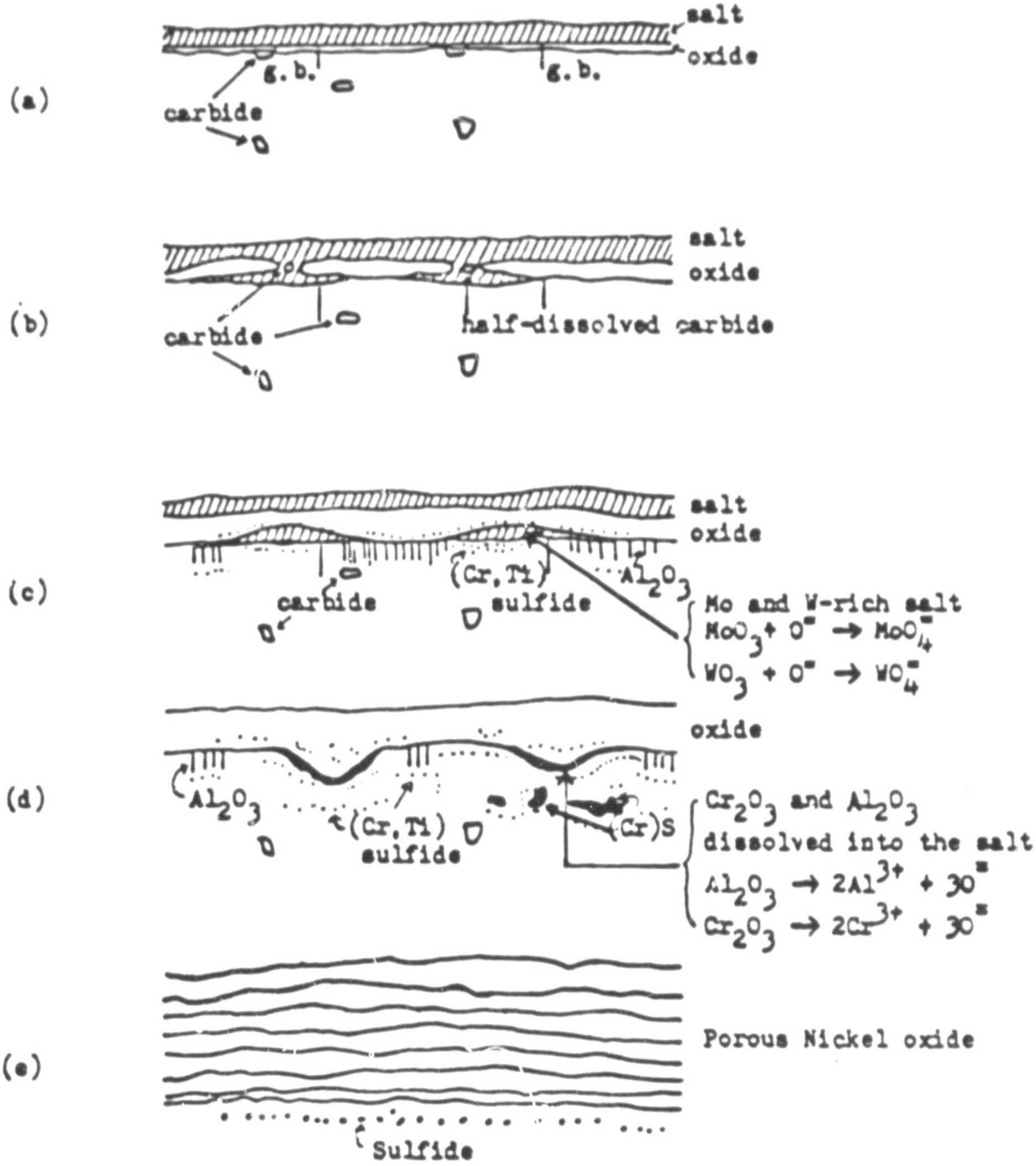

Figure 2 A schematic diagram representing the hot corrosion attack on IN-738-like alloys.

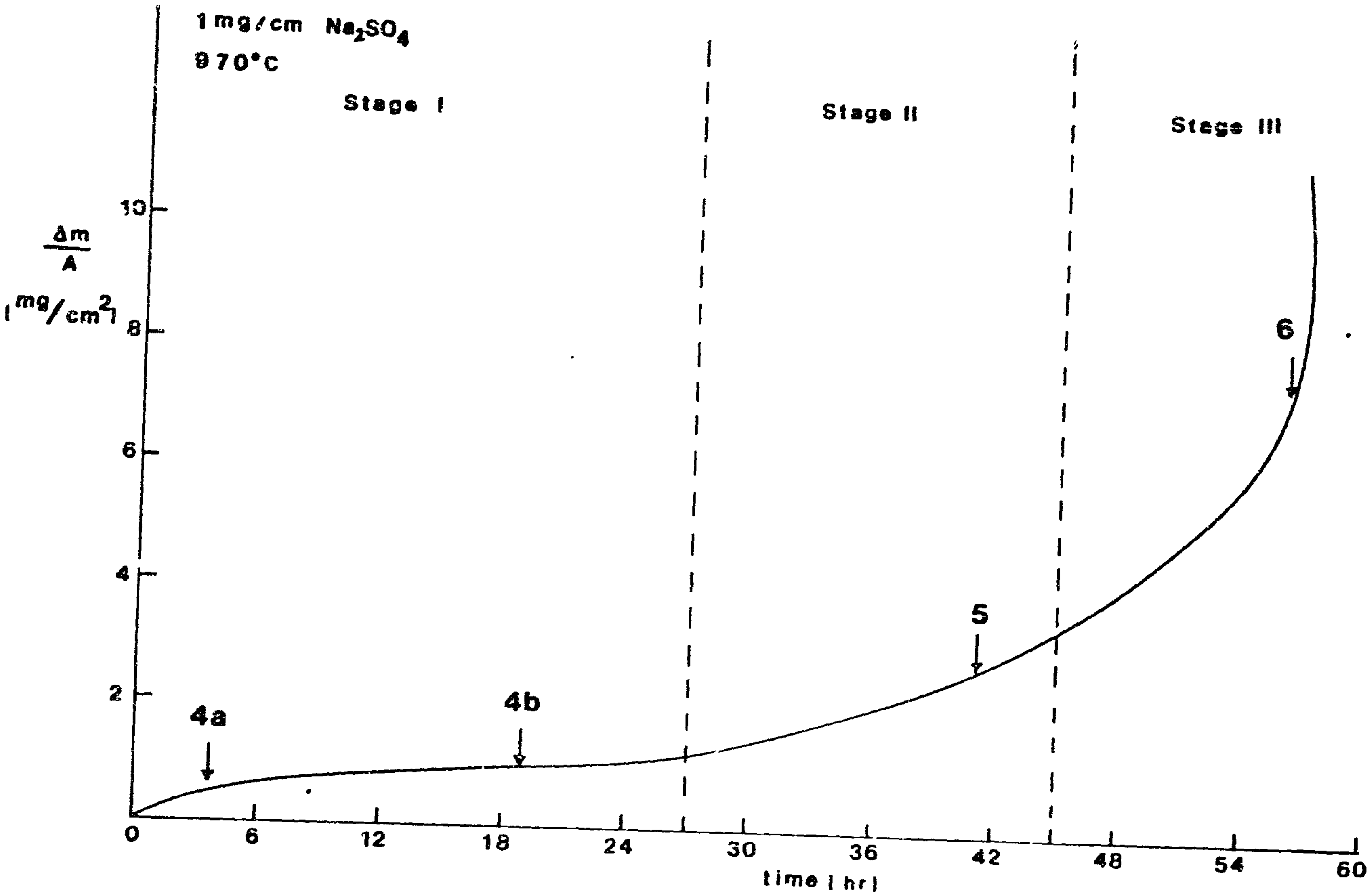

Figure 3. Weight change vs. time for Na_2SO_4-coated IN-738 showing three stages of hot corrosion.

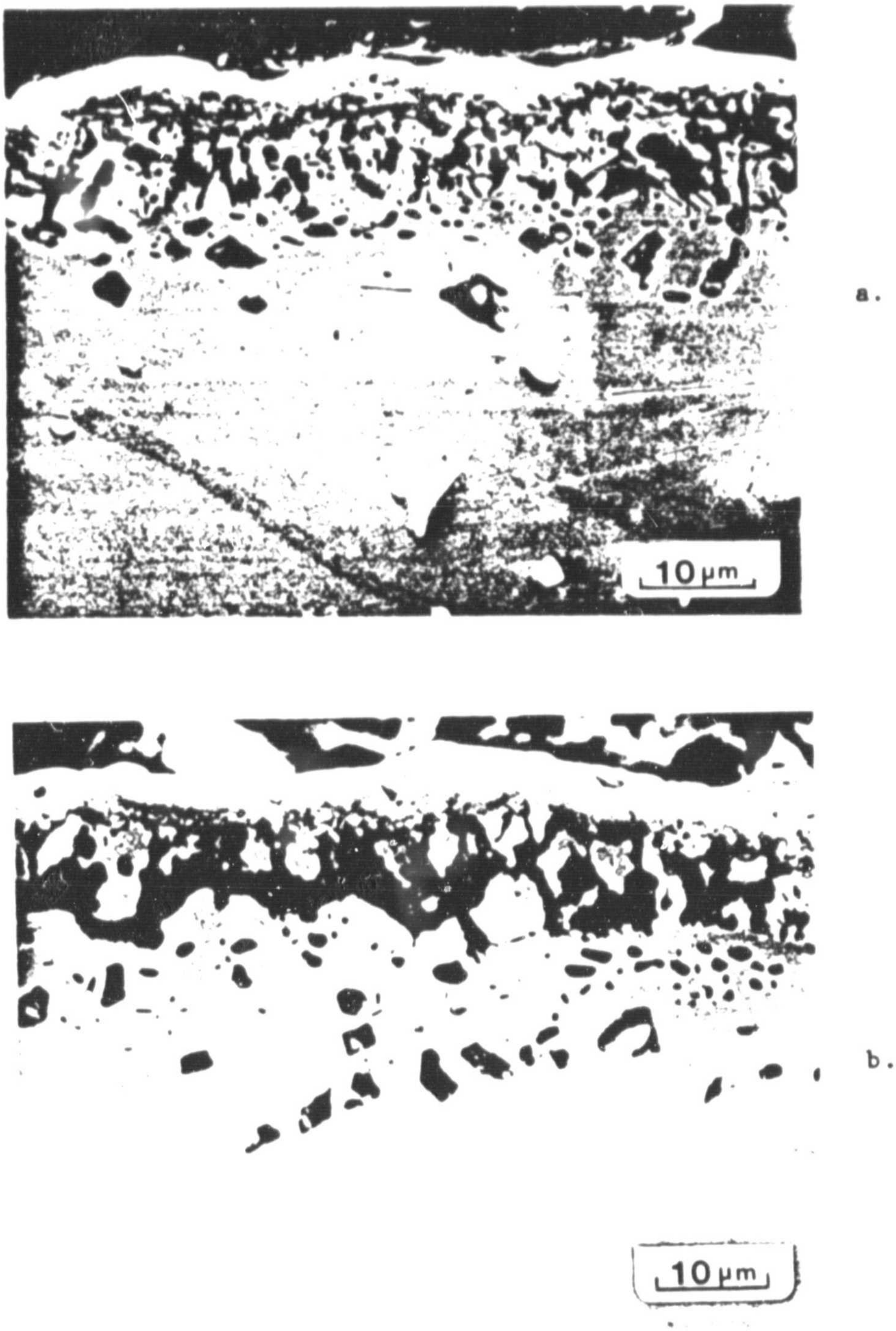

Figure 4 Corrosion morphology during Stage I.

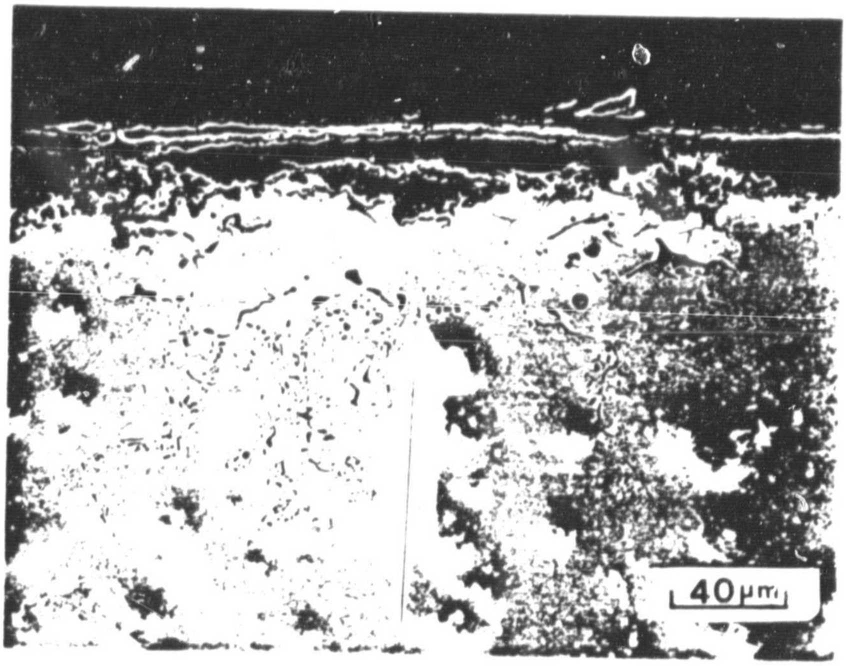

Figure 5 Corrosion morphology during Stage II

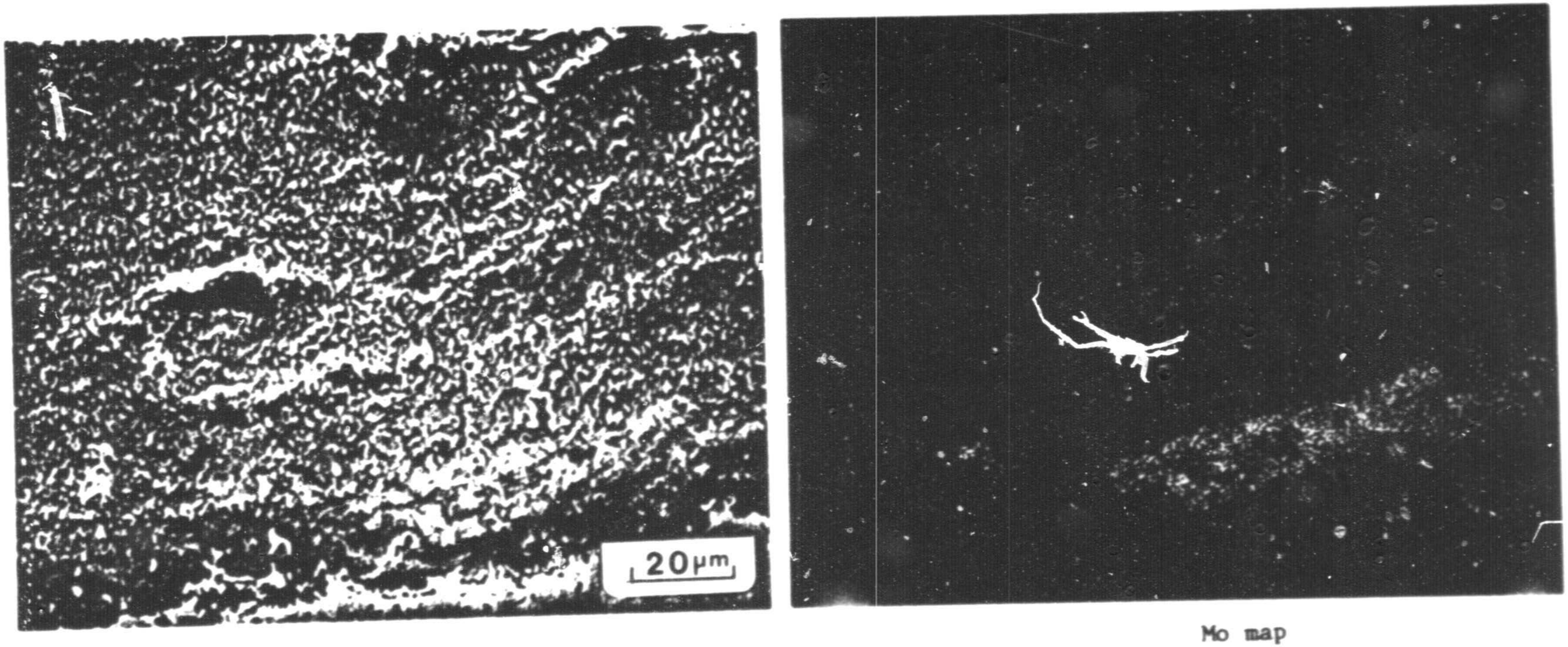

Mo map

Figure 6 Corrosion morphology during Stage II

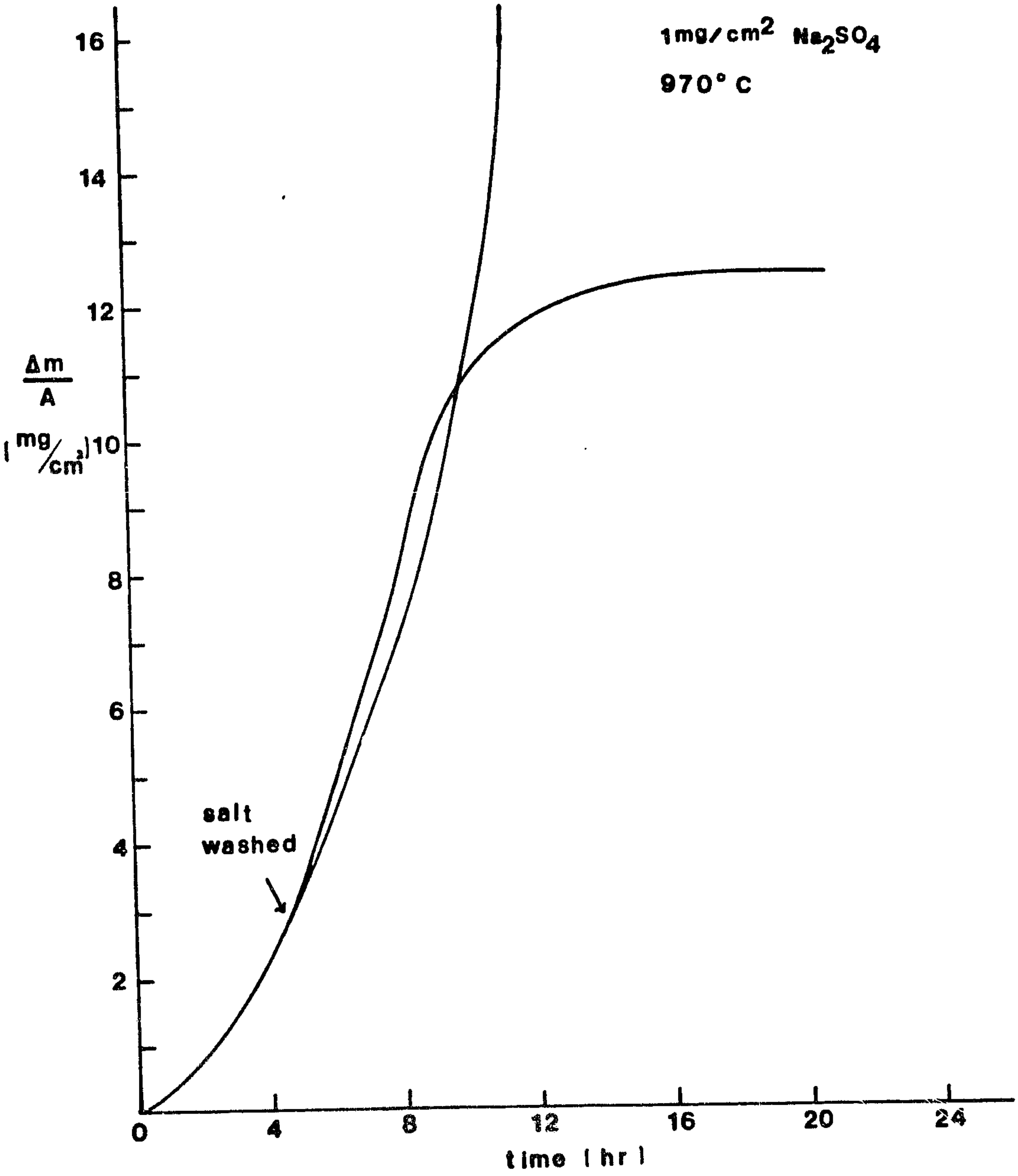

Figure 7 Weight change vs. time for Na_2SO_4-coated IN-738 showing effects of removing the salt during Stage II.

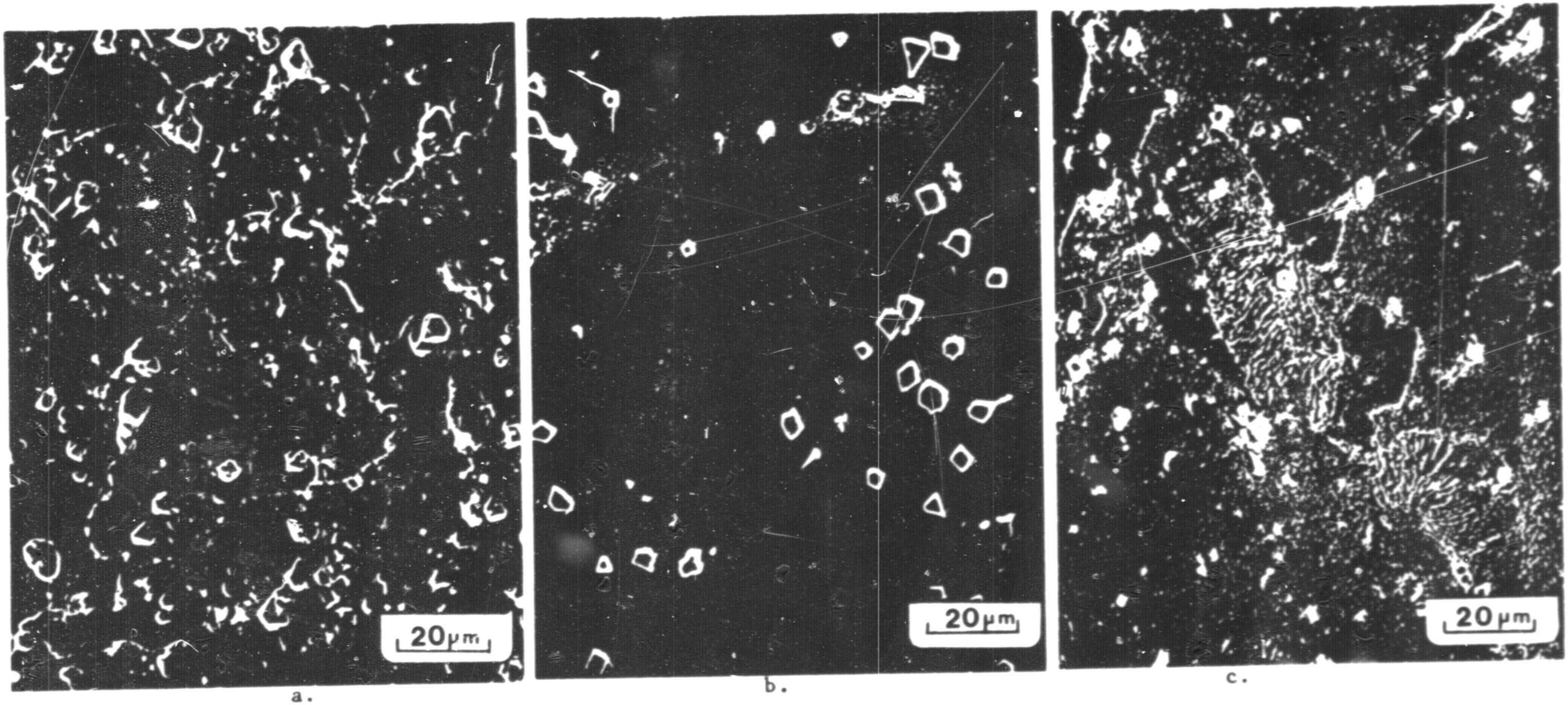

Figure 8 Microstructure of IN-738 specimens cut from three locations in the ingot.

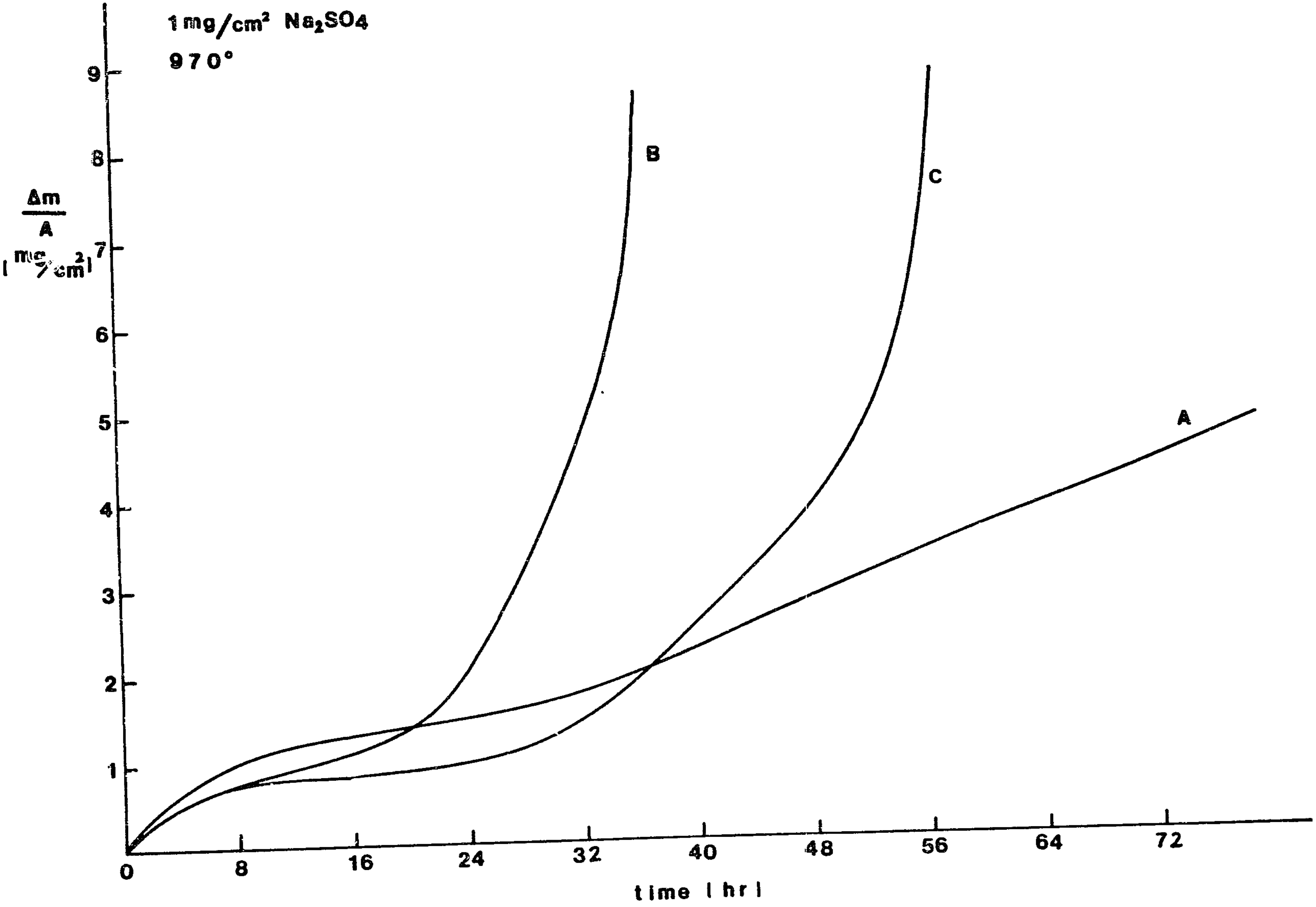

Figure 9 Weight change vs. time for Na_2SO_4-coated specimens cut from three locations in the ingot.